AMERICAN METEOROLOGICAL SOCIETY
45 BEACON STREET
BOSTON, MASSACHUSETTS
02108

TRANSLATION OF

DEVICE FOR MEASURING THE SIZE SPECTRUM OF SPHERICAL PARTICLES AND FOG DROPLETS

(Ustanovka dlia izmereniia spektra razmerov sfericheskikh chastits i kapel' tumanov)

by

V. I. Golikov

Leningrad. Glavnaia Geofizicheskaia Observatoriia, Trudy, No. 109: 76-89, 1961.

This translation has been made by the American Meteorological Society under Contract AF 19(628)-3880, through the support and sponsorship of the

AIR FORCE CAMBRIDGE RESEARCH LABORATORIES

OFFICE OF AEROSPACE RESEARCH

L. G. HANSCOM FIELD

BEDFORD, MASSACHUSETTS

1. "Device for measuring the size spectrum of spherical particles and fog droplets"

2. "Ustanovka dlia izmereniia spektra razmerov sfericheskikh chastits i kapel' tumanov"

3. Golikov, V. I. Leningrad. Glavnaia Geofizicheskaia Observatoriia, Trudy, No. 109: 76-89, 1961.

4. 21 typewritten pages

5. Date of translation: January 1964.

6. Translator: Mahlon Glascock

7. Translated for Air Force Cambridge Research Laboratories, Office of Aerospace Research, United States Air Force, L. G. Hanscom Field, Bedford, Massachusetts, by the American Meteorological Society, Contract number AF 19(628)-3880.

8. Unclassified

9. Complete

DEVICE FOR MEASURING THE SIZE SPECTRUM OF SPHERICAL PARTICLES AND FOG DROPLETS

by

V. I. Golikov

We describe a laboratory device for measuring the size spectrum of spherical particles of powder (plane models of sol) and water droplets (droplets in a thin oil film, and a steam fog in the cloud chamber of the MGO),* and investigate possible sources of error and means of reducing them.

Introduction

Between 1950 and 1955 K. S. Shifrin developed a simple and convenient method for measuring the size spectrum of spherical particles. This method is based on the measurement of the angular distribution of light scattered within a cone of small angle around the direction of propagation of light of the principal light ray. The theory of the method is expounded in [1, 2, 3].

The intensity in direction β is

$$I(\beta) = C\int_0^\infty J_1^2(\rho\beta)\,\rho^2 f(\rho)\,d\rho, \qquad (1)$$

where $f(\rho)$ is the function of the particle size distribution, $J_1(\rho\beta)$ is a first-order Bessel function, $\rho = \frac{2\pi a}{\lambda}$ is a dimensionless radius, associated with wave function λ and particle radius a.

In [2], Shifrin solved the inverse problem by convolution and derived a formula for the spectrum of particle sizes from the intensity distribution of the scattered light

$$f(\rho) = \frac{C^*}{\rho^2}\int_0^\infty \varphi(\beta)\,F(\rho\beta)\,d\beta, \qquad (2)$$

*The A. I. Voeikov Main Geophysical Observatory [Tr. note].

where $\varphi(\beta) \sim \frac{d}{d\beta}(\beta^3 I)$ is derived from $I(\beta)$, which can be determined experimentally

$$F(\rho\beta) = \rho\beta J_1(\rho\beta) Y_1(\rho\beta) \tag{3}$$

which is a tabular function. The tables of function $F(\rho\beta)$ are given in [2]. This paper presents more detailed tables for values of the argument $x = \rho\beta$ from 0 to 10 in steps of 0.01 (see Appendix).

Formula (2) is the basic working formula of the small angle method. If constant C^* is calculated, formula (2) yields both the absolute particle content in the object [investigated] volume and the curve of the size spectrum.

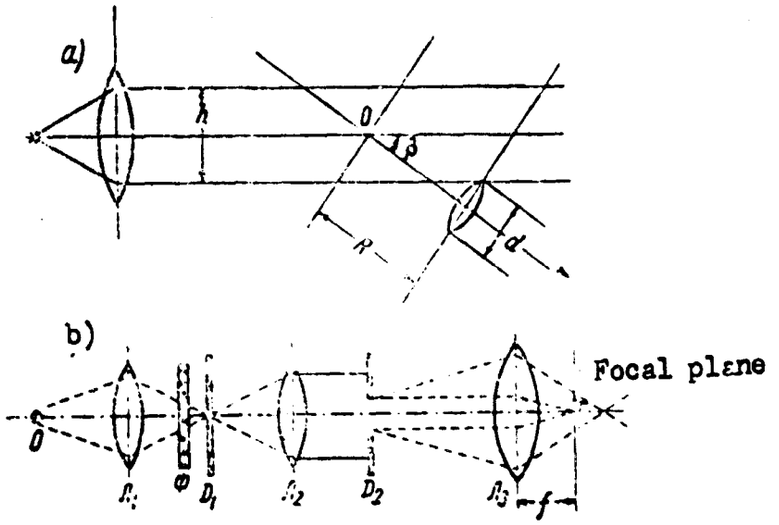

Figure 1

Polar nephelometer (a) and optical system with receiving lens and adjustable diaphragm (b)

The polar nephelometer is not suitable for photometry of the scattering function in a region of small angles. Since scattering angle β is defined here by the formula

$$\beta = \frac{d+h}{2R}, \tag{4}$$

to get small β one must either reduce the beam diameter d or increase the distance between the receiver R and the object

volume (fig. 1a). However, this increases the effect of diffraction, reduces the general sensitivity of the device, and even reduces measurement accuracy. Consequently, at the input of the photometer we installed an optical system consisting of a collimator and a receiving lens; a diaphragm-probe with a small aperture was placed in the focal plane of the lens and could be moved together with the sensing element (photomultiplier) (fig. 1b). The properties of this optical system were described in [4], but the error analysis was based on the investigation of an ideal optical system with a receiving lens and did not consider potential distortion factors in a real system due to spherical aberration, maladjustment of the diaphragm-probe in the focal plane of the receiving lens, misalignment of the optical axes of the illuminator and the receiver, etc.

In this paper we will analyze the possible errors involved in photometry of the scattering function in a region of small angles using a laboratory device constructed in the MGO laboratory. The analysis will be based on the properties of a real optical system.

1. Errors of a real optical system, associated with its geometric parameters

The effect of inaccuracies in determining the geometric parameters of a real system may be evaluated by using the expression for the total luminous flux scattered by particles of a radius ρ in a cone of angle β_n,

$$\Phi(\beta_n) = \pi a^2 \left[1 - J_0^2(\rho\beta_n) - J_1^2(\rho\beta_n)\right], \qquad (5)$$

where β_n is the exact value of scattering angle β, determined by the geometry of the system [4],

$$\beta_n = \frac{\frac{1}{2}l_0}{f}. \qquad (6)$$

where D_o is the diameter of the receiving diaphragm, and f, the focal length of the receiving lens.

The errors involved in bringing the receiving diaphragm into the focus of the lens and the spherical aberration lead to a different value of the angle β_ℓ and, consequently, of the flux $\Phi(\rho\beta_\ell)$. Therefore, we will evaluate the relative errors of determining the scattering angle and the luminous flux

$$\left|\frac{\beta_\ell-\beta_n}{\beta_n}\right|\% \qquad \text{and} \qquad \left|\frac{\Phi_\ell-\Phi_n}{\Phi_n}\right|\%.$$

a. Misalignment of the receiver diaphragm. When the diaphragm is out of the focus of the lens, the cone of the angle of reception for a certain scattering particle L can be determined from fig. 2:

$$[illegible] \qquad (7)$$

where D_s is the diameter of the diaphragm image, ℓ is the distance from point L to the lens, and S' is the distance from the diaphragm image to the lens.

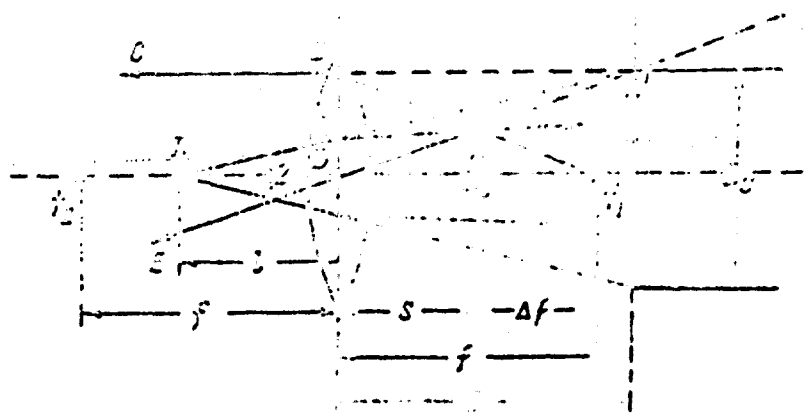

Figure 2

Geometry of the optical system with the diaphragm out of the focus of the lens.

Using the formula for thin lenses, we get

$$[illegible] \qquad (8)$$

Table 1 lists the relative errors $\left|\frac{\beta_\ell - \beta_n}{\beta_n}\right|$ % for lenses with f = 5, 10 and 100 cm, when Δf = 0.01, 0.1, 0.5 and 1.0 cm. Angle $\beta_n = 1^\circ$, and distance ℓ = 1, 10, 50 cm.

The calculations show that for average values of ρ, a 0.5% change in $\Phi(\rho\beta)$ corresponds roughly to a 1% change in β. Therefore, table 1 can be used to determine the errors which the misalignment of the diaphragm introduces into the photometrically determined distribution curves of scattered light.

Table 1

ℓ cm	Δf cm	f = 5 cm		f = 10 cm		f = 100 cm	
		ζ	$\left\|\frac{\beta_\ell - \beta_n}{\beta_n}\right\|$ %	ζ	$\left\|\frac{\beta_\ell - \beta_n}{\beta_n}\right\|$ %	ζ	$\left\|\frac{\beta_\ell - \beta_n}{\beta_n}\right\|$ %
1	0,01	0,002	0,16	0,001	0,1	0,0001	0,0
1	0,1	0,02	1,6	0,01	0,9	0,001	0,1
1	0,5	0,1	8,7	0,05	4,7	0,005	0,5
1	1,0	0,2	19,1	0,1	9,9	0,01	1,0
10	0,01	0,002	1,2	0,001	0,0	0,0001	0,01
10	0,1	0,02	1,6	0,01	0,0	0,001	0,1
10	0,5	0,1	9,1	0,05	0,0	0,005	0,4
10	1,0	0,2	16,7	0,1	0,0	0,01	0,9
50	0,01	0,002	1,8	0,001	0,1	0,0001	0,01
50	0,1	0,02	15,3	0,01	3,5	0,001	0,1
50	0,5	0,1	47,4	0,05	16,7	0,005	0,55
50	1,0	0,2	61,3	0,1	28,6	0,01	0,5

As in [4], our models of a plane sol have $\ell \to 0$ and the length of the illuminated volume of fog $\ell \leq 15$ cm. Since angle β did not exceed 3 to 5° and f = 30, 50, and 93 cm, the corresponding calculations indicate that the permissible misalignment of the diaphragm $\Delta f = \pm 0.5$ to 1 cm.

b. Spherical aberration. Spherical aberration causes paraxial and nonparaxial light beams to focus at different points. Third-order aberration theory provides the following expression for the focusing error of Δf [5]

$$\Delta f = S'S'_t = \frac{r_1}{f'} Q(n, p, q), \qquad (9)$$

where S' is the image distance for paraxial rays; S'_r the image distance for a ray passing through the lens at distance r from the optical axis; f is the paraxial focus; n, the refractive index (n = 1.5); and $p = \frac{S' - S}{S' + S} = -1$ (S is the distance to the lens and, in our case, is indeterminate).

Generally, Δf is small; therefore, $S' = f$, $S'_r \approx f$, and

$$\Delta f \sim \frac{r^2}{f} \cdot \frac{n+2}{2(n-1)} \qquad (10)$$

Having assumed a focus $f + \Delta f$ and using (7), (8), we get

$$\Delta f \sim \frac{d^2}{16 f Q} \qquad (11)$$

where d is the diameter of the light beam.

Since $f^2 - r^2 Q \approx f^2$, for the relative error due to spherical aberration we get

$$\frac{\Delta f}{f} \sim \frac{1}{16 f^2 Q} \qquad (12)$$

For a biconvex lens [5], Q = 1.5 when n = 1.5 and q = 0. Finally

$$\frac{\Delta f}{f} \sim \frac{d^2}{24 f^2} \qquad (13)$$

Table 2 presents the results of calculations by formula (13) for lenses with f = 5, 10 and 100 cm, when the diameter of the primary light beam d = 0.5, 1.0, 2.0, 2.5 cm and ℓ_{max} = 1, 10 and 50 cm.

The table shows that for polydisperse systems with $\ell \leq 15$ cm, as described in [4], spherical aberration may be neglected even for lenses with f ~ 10 cm.

c. <u>Divergence of the principal light beam</u>. The calculations show that the residual divergence of the parallel beam may be made negligibly small, e.g., to 1 to 3'.

Table 2

1	0,3	0,0		0,0
	1,0	0,2		0,0
	2,0	0,2		0,0
	2,3	0		0,0
				0,0
	1,0	0,5		0,0
	2,0			0,0
10	2,3	4,7	0,0	0,0
		0,9		0,0
				0,0
	2,0			0,0
		22,8		0,0

d. Misalignment of the optical axes of the receiver and the illuminator. This type of error affects the absolute value of the intensity of the scattered light, but not the shape of the curve (provided the investigated polydisperse medium is statistically homogeneous). Therefore, this misalignment may also be neglected in relative measurements of $f(\rho)$ and relative accuracies of photometry of $I(\beta)$, such as those in [4].

The last two types of geometric errors of an optical system with a lens and a point diaphragm reinforce one another and they must be determined more exactly in an absolute analysis of the microstructure of the sol.

Thus, our evaluations of the geometric errors indicate that the optical system with a lens is a good approximation of the ideal system for the sol models examined in [4].

2. Laboratory Apparatus

We constructed the principal optical system (fig. 1) at the MGO as a stationary laboratory version for working with

plane models of calibrated sol (drops of water in a thin oil film, and powders on a glass slide) and a portable version for working in fog. Figure 3 shows the stationary version. Light source 1 (mercury-vapor lamp SVDSh-250-3), condensing lens 2 with f = 9 cm, point diaphragm 3 with a 0.1 to 0.5 mm diameter, collimator lens 4 with f = 20 cm and a light filter at λ = 546 mμ comprise the source of the monochromatic parallel light beam. Behind the output diaphragm 5, which adjusts the diameter of the beam, is a plane sol sample 6 mounted on a device which rotates it in a plane perpendicular to the direction of propagation of the light, in order to reduce the possible statistical inhomogeneity of the sample [4]. Lens 7 with f = 35, 50 or 93 cm, and photomultiplier 9 with point diaphragm 8 receive the scattered light. The light receiver is moved by a micrometer screw and an SD-2 motor 10 in the focal plane of lens 7. The illustration shows the control panel 11 of the photometer and the K4-51 photorecorder 12 (a PSR-01 potentiometer may be used in place of the K4-51).

For the parameters of the optical components indicated here, the device has a resolution of 2.5 to 5' at angle β which assures a critical angle of approach to the zero direction of $\beta_{crit} \approx 13'$. The maximum angle of capture of the scattered light is about 3 to 5°. It takes 10 to 15 min (with PSR-01) to record the full curve of $I(\beta)$. The sensitivity of the photometer with the dc amplifier enables it to measure luminous fluxes up to 10^{-9} lu with an accuracy of at least 10 to 15%.

The device is located in a special photometric room and all measurements are made in total darkness.

The portable version for work in the cloud chamber consists of an illuminator and a "Kiev 3" camera. The illuminator (a headlight with a condenser, a point diaphragm, an interference filter at λ = 546 mμ and a collimator lens) is mounted on a theolodite tripod. Standard 35-mm film is used

as the light receiver. The negatives are measured on an MF-4 microphotometer at an increased magnification [4].

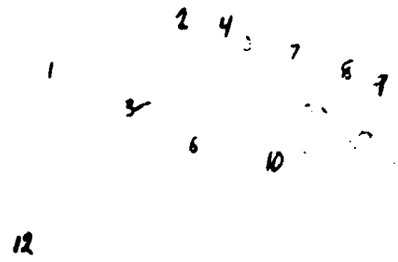

Figure 3

General view of the stationary apparatus for analyzing the microstructure of the sol.

3. Possible sources of systematic errors and methods of reducing them

In addition to the errors in determining the geometric parameters indicated in sec. 1, the following sources of error may appear in the experimental curves of the distribution of scattered light: fluctuations of the output illuminator, non-monochromatic light, foreign matter in the optics, parasitic reflections in the optics, fluctuations of the power supply, noises of the photomultiplier and the amplifier (when the photoelectric method of photometry is employed), and errors in the photographic method of measuring $I(\beta)$.

These sources of systematic errors can be reduced by adjusting the optical system and calibrating the photometer and the film during actual measurement.

The luminous flux from the SVDSh-250-3 can be stabilized as desired with a ferro-resonance stabilizer, and the current regulator tubes, by current stabilizers.

The use of a narrow-band interference filter on the mercury line at $\lambda = 546$ mμ virtually insures a monochromatic principal light beam.

The reflections were most noticeable when working with cuvettes and plane models in the area between the receiving lens and the sol sample; their effect was eliminated by slightly inclining the plane of the sample toward the plane of the lens or by increasing the distance between the lens and the sample.

The influence of foreign matter on the optics is generally a combination of parasitic light scattering in air (by the dust suspended in it) and dirt on the lens. This produces a so-called "zero distribution," $I_o(\beta)$, i.e., the light scattering of the system itself. To exclude $I_o(\beta)$, photometry is carried out twice, with and without the sol, and the ordinates of the light scattering curves are subtracted (of course, with allowance for attenuation). The difference curve gives an $I(\beta)$ corresponding to the investigated particles.

The photometer supply is stabilized in two ways: by a ferro-resonance stabilizer for the supply voltage and by an electronic stabilizer for the high voltage of the photomultiplier and the anodes of the amplifier tubes. The tubes are heated by high-capacitance storage batteries. If the dc amplifier is allowed to heat up for an hour, these stabilizers limit its variation to 0.5 of the smallest scale division of the output device (microammeter) over a ten-minute period.

The real difficulty in using the photometer is the large decrease of intensity values ($I_o/I_{min} = 10^3 - 10^6$) in the investigated region of angles $\beta = 3$ to 5^o [4]. Consequently, the

accuracy of photometry along β is inconsistent. The effect of the photomultiplier's electrical noises and the dark current increases at β_{max}.

The photometer parameters were selected so that luminous fluxes of 10^{-9} lu could be measured to an accuracy of at least 10 to 15%, and this accuracy may be increased by refining the electrical circuit of the photometer.

The photographic method introduces familiar difficulties: errors due to the nonlinearity of the characteristic curve of the blackening of the film, the dispersion halo in the emulsion, microdensitometer errors, the dependence of the quality of the negatives upon the method of chemical development, etc. For our conditions, we attained a 20% accuracy of photographic photometry.

The photometry of the scattering functions at small angles using our laboratory device yields a high accuracy of measuring $I(\beta)$, which is at least 10 to 15% for the photoelectric and 20 to 25% for the photographic method of measuring illumination.

The experimental curves may be integrated on graphs according to formula (2) to an accuracy of 5 to 10%, depending on the extent to which the tabular and graphic data are used, and the training of the computer engineer [4].

We took the sum of errors in the photometry and the graph integration as the final accuracy of calculating the ordinates of the size-spectrum curve $f(\rho)$ and obtained 20 to 25% for the photoelectric and 25 to 30% for the photographic method.

4. Comparison of the experimental results with a photomicrographic count of the particles

Figure 4 gives a general view of the photic fields and the corresponding distributions of illumination for plane models of sol and fog droplets.

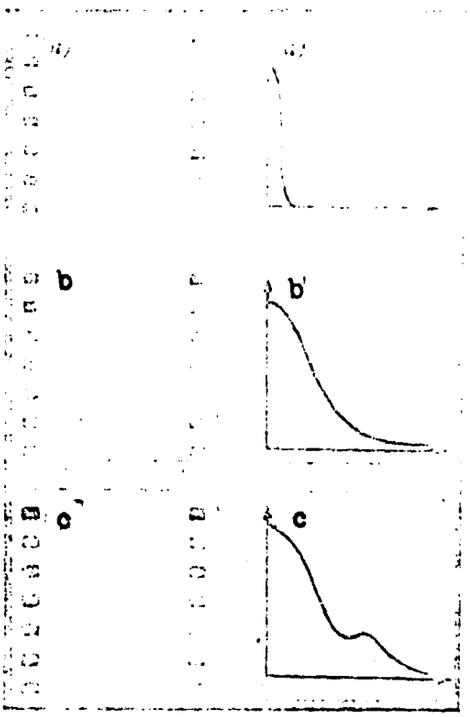

Figure 4

View of photic fields in the focal plane of the receiving lens and the curves of the distribution of illumination corresponding to them.

a. zero distribution; b. fog droplets
c. lycopodium spores

In [4] we presented the data of the graphic processing of the curves of $I(\beta)$, and, therefore, we will present only the final size spectrum of $f(a)$, in fig. 5, which compares curves of particle-size spectra, obtained by the small-angle method, with histograms of a direct particle count using photomicrography.

The errors in comparing the results of these two methods of analyzing the microstructure of the sol are chiefly statistical. The largest number of counted particles (up to 3000 per model) and photometrically measured curves $I(\beta)$ were obtained for the plane models, thus the agreement of the size-spectrum curves in fig. 5a-e (plane models) may be considered good. The agreement is not as good for fog droplets because of the large error in the photographic photometry of

the scattering functions (for the size spectrum near the lower limit of the small-angle method) and because of possible distortions in the structure of the fog samples taken for photomicrography.

Conclusion

1. The results of analysis in sec. 1 showed that the properties of the laboratory device for working with the plane models and fog described by us [4] and in this paper, closely approximate those of an ideal optical system.

2. For absolute photometry and design calculations of a field apparatus based on the small-angle method, one must also analyze the errors involved in determining the geometric parameters of a real optical system with a receiving lens and a point diaphragm (sec. 1). This problem will be treated in a special paper.

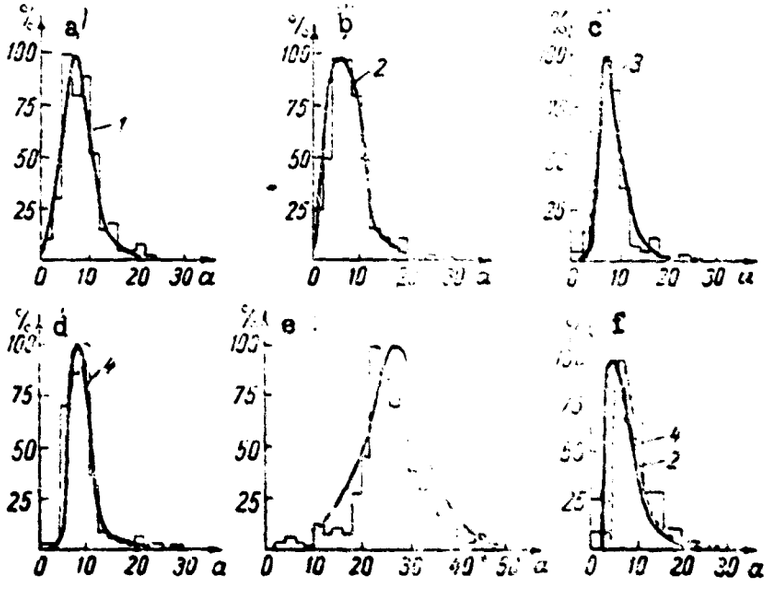

Figure 5

Comparison of the size spectra obtained by the small-angle method and by photomicrography.

a to e. plane models of sol; f. fog droplets.

3. The main experimental errors are errors of photometry, and, thus, to improve these results the photometer must be improved.

4. Errors in graph processing of the experimental curves $I(\beta)$ are unavoidable. To facilitate calculations, more complete tables for function $F^{x}(\rho\beta)$ are presented (see Appendix), whose values were grouped by fixed values of ρ.

5. A comparison of the small-angle method with the direct-count method shows them to be in good agreement for statistically homogeneous systems. In photometry of a spatially inhomogeneous sol, measures must be taken to obtain a scattering function averaged over the entire illuminated volume.

LITERATURE CITED

1. Shifrin, K. S. Rasseianie sveta v mutnoi srede (Light scattering in a turbid medium). Gostekhizdat, 1951.

2. Shifrin, K. S. "Vychislenie nekotorogo klassa opredelennykh integralov, soderzhashchikh kvadrat besselevoi funktsii pervogo poriadka" (Calculation of a certain class of definite integrals containing the square of a first-order Bessel function), Leningrad. Vsesoiuznyi Zaochnyi Lesotekhnicheskii Institut, Trudy, No. 2, 1956.

3. Shifrin, K. S. "Opticheskie issledovaniia oblachnykh chastits" (Optical investigations of cloud particles), in: Issledovanie oblakov, osadkov i grozovogo elektrichestva (Investigation of clouds, precipitation and thunderstorm electricity). Gidrometeoizdat, 1957.

4. Shifrin, K. S. and V. I. Golikov. "Opredelenie spektra kapel' metodom malykh uglov" (Determination of droplet spectra by the small-angles method), in: Vul'fson, N. I. and L. M. Levin (eds.) Issledovaniia oblakov, osadkov i grozovogo elektrichestva (Investigations of clouds, precipitation and thunderstorm electricity), Moscow, Izd-vo Akademii Nauk SSSR, 1961. pp. 266-277.

5. Tudorovskii, A. I. Teoriia opticheskikh priborov (Theory of optical instruments), Vol. I, Moscow, Izd-vo Akademii Nauk SSSR, 1948.

APPENDIX

Table of function F(x)

Table of function F(x)

x	F (x)	x	F (x)	x	F (x)	x	F (x)
0,00	0,0000	0,51	0,1824	1,01	0,3459	1,51	—0,3127
		0,52	1863	1,02	3479	1,52	3102
0,01	—0,0032	0,53	1901	1,03	3499	1,53	3076
0,02	0,0064	0,54	1939	1,04	3518	1,54	3050
0,03	0096	0,55	—0,1976	1,05	—0,3536	1,55	—0,3022
0,04	0127						
0,05	—0,0160	0,56	—0,2015	1,06	—0,3554	1,56	—0,3293
		0,57	2053	1,07	3571	1,57	3261
0,06	—0,0192	0,58	2092	1,08	3587	1,58	3233
0,07	0225	0,59	2130	1,09	3602	1,59	3202
0,08	0257	0,60	—0,2168	1,10	—0,3616	1,60	—0,3169
0,09	0290						
0,10	—0,0322	0,61	—0,2206	1,11	—0,3630	1,61	—0,3135
		0,62	2244	1,12	3643	1,62	3102
0,11	—0,0356	0,63	2281	1,13	3654	1,63	3067
0,12	0389	0,64	2320	1,14	3666	1,64	3031
0,13	0422	0,65	—0,2357	1,15	—0,3676	1,65	—0,2994
0,14	0456						
0,15	—0,0490	0,66	—0,2394	1,16	—0,3684	1,66	—0,2956
		0,67	2131	1,17	3694	1,67	2918
0,16	—0,0524	0,68	2468	1,18	3701	1,68	2878
0,17	0558	0,69	2501	1,19	3708	1,69	2838
0,18	0592	0,70	—0,2541	1,20	—0,3714	1,70	—0,2797
0,19	0630						
0,20	—0,0661	0,71	—0,2577	1,21	0,3719	1,71	—0,2755
		0,72	2612	1,22	3723	1,72	2712
0,21	—0,0696	0,73	2648	1,23	3726	1,73	2668
0,22	0732	0,74	2683	1,24	3728	1,74	2624
0,23	0767	0,75	—0,2719	1,25	—0,3730	1,75	2578
0,24	0803						
0,25	—0,0838	0,76	—0,2752	1,26	—0,3730	1,76	—0,2533
		0,77	2786	1,27	3730	1,77	2486
0,26	—0,0874	0,78	2820	1,28	3728	1,78	2438
0,27	0911	0,79	2853	1,29	3726	1,79	2390
0,28	0947	0,80	—0,2885	1,30	—0,3722	1,80	—0,2341
0,29	0984						
0,30	—0,1020	0,81	—0,2919	1,31	—0,3718	1,81	—0,2292
		0,82	2951	1,32	3713	1,82	2241
0,31	—0,1057	0,83	2983	1,33	3707	1,83	2190
0,32	1094	0,84	3014	1,34	3699	1,84	2138
0,33	1132	0,85	—0,3044	1,35	—0,3691	1,85	—0,2086
0,34	1169						
0,35	—0,1207	0,86	—0,3074	1,36	—0,3682	1,86	—0,2033
		0,87	3101	1,37	3672	1,87	1980
0,36	—0,1244	0,88	3130	1,38	3661	1,88	1926
0,37	1282	0,89	3162	1,39	3648	1,89	1871
0,38	1320	0,90	—0,3186	1,40	—0,3636	1,90	—0,1806
0,39	1358						
0,40	—0,1396	0,91	—0,3218	1,41	—0,3621	1,91	—0,1771
		0,92	3244	1,42	3606	1,92	1703
0,41	—0,1435	0,93	3271	1,43	3590	1,93	1646
0,42	1473	0,94	3296	1,44	3573	1,94	1589
0,43	1512	0,95	—0,3322	1,45	—0,3555	1,95	—0,1531
0,44	1550						
0,45	—0,1588	0,96	—0,3345	1,46	—0,3538	1,96	—0,1473
		0,97	3370	1,47	3516	1,97	1414
0,46	—0,1627	0,98	3393	1,48	3493	1,98	1354
0,47	1666	0,99	3416	1,49	3471	1,99	1295
0,48	1705	1,00	—0,3438	1,50	—0,3447	2,00	—0,1234
0,49	1744						
0,50	—0,1783						

x	$F(x)$	x	$F(x)$	x	$F(x)$	x	$F(x)$
2,01	—0,1174	2,53	0,1969	3,04	0,3301	3,56	0,1653
2,02	1113	2,54	2019	3,05	0,3297	3,57	1598
2,03	1052	2,55	0,2069			3,58	1542
2,04	0991			3,06	0,3293	3,59	1485
2,05	—0,0929	2,56	0,2118	3,07	3287	3,60	0,1428
		2,57	2166	3,08	3279		
2,06	—0,0867	2,58	2214	3,09	3271	3,61	0,1370
2,07	0805	2,59	2260	3,10	0,3262	3,62	1312
2,08	0742	2,60	0,2306			3,63	1253
2,09	0680			3,11	0,3251	3,64	1190
2,10	—0,0617	2,61	0,2360	3,12	3239	3,65	0,1134
		2,62	2395	3,13	3226		
2,11	—0,0554	2,63	2438	3,14	3211	3,66	0,1074
2,12	0490	2,64	2480	3,15	0,3196	3,67	1014
2,13	0427	2,65	0,2522			3,68	0953
2,14	0321			3,16	0,3179	3,69	0891
2,15	—0,0300	2,66	0,2572	3,17	3161	3,70	0,0830
		2,67	2601	3,18	3142		
2,16	—0,0236	2,68	2640	3,19	3122	3,71	0,0768
2,17	0173	2,69	2678	3,20	0,3100	3,72	0706
2,18	0109	2,70	0,2714			3,73	0644
2,19	0046			3,21	0,3078	3,74	0581
2,20	0,0018	2,71	0,2750	3,22	3054	3,75	0,0518
		2,72	2784	3,23	3029		
2,21	0,0082	2,73	2818	3,24	3003	3,76	0,0455
2,22	0145	2,74	2850	3,25	0,2976	3,77	0392
2,23	0209	2,75	0,2882			3,78	0329
2,24	0272			3,26	0,2948	3,79	0265
2,25	0,0336	2,76	0,2912	3,27	2919	3,80	0,0202
		2,77	2942	3,28	2888		
2,26	0,0399	2,78	2970	3,29	2857	3,81	0,0138
2,27	0462	2,79	2997	3,30	0,2824	3,82	0074
2,28	0524	2,80	0,3023			3,83	0,0042
2,29	0587			3,31	0,2791	3,84	—0,0053
2,30	0,0649	2,81	0,3048	3,32	2756	3,85	—0,0116
		2,82	3072	3,33	2721		
2,31	0,0711	2,83	3095	3,34	2684	3,86	—0,0180
2,32	0773	2,84	3117	3,35	0,2646	3,87	0243
2,33	0834	2,85	0,3137			3,88	0307
2,34	0896			3,36	0,2608	3,89	0370
2,35	0,0956	2,86	0,3156	3,37	2568	3,90	—0,0433
		2,87	3173	3,38	2528		
2,36	0,1017	2,88	3192	3,39	2486	3,91	—0,0496
2,37	1077	2,89	3196	3,40	0,2444	3,92	0559
2,38	1136	2,90	0,3222			3,93	0622
2,39	1196			3,41	0,2400	3,94	0684
2,40	0,1254	2,91	0,3238	3,42	2366	3,95	—0,0746
		2,92	3248	3,43	2311		
2,41	0,1313	2,93	3259	3,44	2265	3,96	—0,0808
2,42	1371	2,94	3267	3,45	0,2218	3,97	0869
2,43	1428	2,95	0,3277			3,98	0930
2,44	1485			3,46	0,2171	3,99	0991
2,45	0,1541	2,96	0,3285	3,47	2122	4,00	—0,1051
		2,97	3291	3,48	2073		
2,46	0,1597	2,98	3296	3,49	2023	4,01	—0,1111
2,47	1649	2,99	3300	3,50	0,1972	4,02	1168
2,48	1706	3,00	0,3302			4,03	1230
2,49	1760			3,51	0,1921	4,04	1288
2,50	0,1813	3,01	0,3304	3,52	1869	4,05	—0,1316
		3,02	3304	3,53	1816		
2,51	0,1866	3,03	3303	3,54	1762	4,06	—0,1404
2,52	1918			3,55	0,1708	4,07	1461

x	$F(x)$	x	$F(x)$	x	$F(x)$	x	$F(x)$
4,08	−0,1517	4,61	−0,3231	5,13	−0,1800	5,66	0,1436
4,09	1573	4,62	3236	5,14	1750	5,67	1472
4,10	−0,1628	4,63	3237	5,15	−0,1693	5,68	1528
		4,64	3236			5,69	1584
4,11	−0,1683	4,65	−0,3235	5,16	−0,1638	5,70	0,1639
4,12	1737			5,17	1583		
4,13	1790	4,66	−0,3232	5,18	1527	5,71	0,1693
4,14	1843	4,67	3227	5,19	1488	5,72	1745
4,15	−0,1895	4,68	3222	5,20	−0,1413	5,73	1807
		4,69	3215			5,74	1857
4,16	−0,1945	4,70	−0,3207	5,21	−0,1356	5,75	0,1907
4,17	1997			5,22	1300		
4,18	2046	4,71	−0,3198	5,23	1239	5,76	0,1956
4,19	2094	4,72	3188	5,24	1180	5,77	2005
4,20	−0,2152	4,73	3176	5,25	−0,1123	5,78	2055
		4,74	3163			5,79	2103
4,21	−0,2190	4,75	−0,3149	5,26	−0,1061	5,80	0,2152
4,22	2237			5,27	1000		
4,23	2282	4,76	−0,3133	5,28	0959	5,81	0,2198
4,24	2327	4,77	3117	5,29	0878	5,82	2247
4,25	−0,2371	4,78	3098	5,30	−0,0817	5,83	2299
		4,79	3080			5,84	2335
4,26	−0,2413	4,80	−0,3060	5,31	−0,0755	5,85	0,2376
4,27	2455			5,32	0693		
4,28	2496	4,81	−0,3039	5,33	0631	5,86	0,2419
4,29	2536	4,82	3016	5,34	0586	5,87	2460
4,30	−0,2575	4,83	2992	5,35	−0,0505	5,88	2501
		4,84	2967			5,89	2540
4,31	−0,2613	4,85	−0,2942	5,36	−0,0442	5,90	0,2579
4,32	2650			5,37	0379		
4,33	2686	4,86	−0,2920	5,38	0316	5,91	0,2618
4,34	2721	4,87	2896	5,39	0252	5,92	2652
4,35	−0,2755	4,88	2857	5,40	−0,0189	5,93	2688
		4,89	2826			5,94	2722
4,36	−0,2788	4,90	−0,2795	5,41	−0,0125	5,95	0,2756
4,37	2820			5,42	0062		
4,38	2850	4,91	−0,2762	5,43	0,00002	5,96	0,2788
4,39	2880	4,92	2728	5,44	0066	5,97	2819
4,40	−0,2908	4,93	2691	5,45	0,0129	5,98	2850
		4,94	2658			5,99	2878
4,41	−0,2936	4,95	−0,2621	5,46	0,0193	6,00	0,2907
4,42	2962			5,47	0256		
4,43	2987	4,96	−0,2582	5,48	0320	6,01	0,2935
4,44	3012	4,97	2541	5,49	0383	6,02	2963
4,45	−0,3034	4,98	2501	5,50	0,0446	6,03	2990
		4,99	2460			6,04	3015
4,46	−0,3055	5,00	−0,2422	5,51	0,0509	6,05	0,3027
4,47	3076			5,52	0572		
4,48	3095	5,01	−0,2379	5,53	0634	6,06	0,3018
4,49	3113	5,02	2336	5,54	0697	6,07	3067
4,50	−0,2130	5,03	2291	5,55	0,0759	6,08	3086
		5,04	2239			6,09	3103
4,51	−0,3145	5,05	−0,2199	5,56	0,0820	6,10	0,3119
4,52	3160			5,57	0882		
4,53	3173	5,06	−0,2152	5,58	0943	6,11	0,3133
4,54	3185	5,07	2101	5,59	1003	6,12	3147
4,55	−0,3196	5,08	2055	5,60	0,1064	6,13	3159
		5,09	2006			6,14	3170
4,56	−0,3205	5,10	−0,1955	5,61	0,1123	6,15	0,3180
4,57	3213			5,62	1183		
4,58	3220	5,11	−0,1904	5,63	1242	6,16	0,3189
4,59	3226	5,12	1852	5,64	1300	6,17	3196
4,60	−0,3231			5,65	0,1358		

x	$F(x)$	x	$F(x)$	x	$F(x)$	x	$F(x)$
6,18	0,3202	6,71	0,1829	7,23	0,1624	7,76	−0,3189
6,19	3207	6,72	1776	7,24	1582	7,77	3194
6,20	0,3210	6,73	1723	7,25	−0,1539	7,78	3198
		6,74	1669			7,79	3201
6,21	0,3212	6,75	0,1614	7,26	0,1495	7,80	−0,3202
6,22	3213			7,27	1551		
6,23	3213	6,76	0,1556	7,28	1607	7,81	−0,3202
6,24	3211	6,77	1503	7,29	1661	7,82	3201
6,25	0,3209	6,78	1446	7,30	−0,1715	7,83	3199
		6,79	1389			7,84	3195
6,26	0,3205	6,80	0,1331	7,31	−0,1769	7,85	−0,3190
6,27	3199			7,32	1822		
6,28	3193	6,81	0,1273	7,33	1874	7,86	−0,3184
6,29	3185	6,82	1214	7,34	1917	7,87	3176
6,30	0,3176	6,83	1155	7,35	−0,1975	7,88	3168
		6,84	1096			7,89	3158
6,31	0,3165	6,85	0,1036	7,36	−0,2025	7,90	−0,3147
6,32	3154			7,37	2074		
6,33	3141	6,86	0,0975	7,38	2122	7,91	−0,3134
6,34	3127	6,87	0914	7,39	2167	7,92	3120
6,35	0,3112	6,88	0853	7,40	−0,2216	7,93	3105
		6,89	0791			7,94	3089
6,36	0,3095	6,90	0,0730	7,41	−0,2261	7,95	−0,3072
6,37	3078			7,42	2305		
6,38	3059	6,91	0,0667	7,43	2349	7,96	−0,3053
6,39	3039	6,92	0605	7,44	2392	7,97	3034
6,40	0,3017	6,93	0542	7,45	−0,2434	7,98	3013
		6,94	0480			7,99	2990
6,41	0,2995	6,95	0,0416	7,46	−0,2475	8,00	−0,2967
6,42	2971			7,47	2515		
6,43	2947	6,96	0,0353	7,48	2553	8,01	−0,2942
6,44	2920	6,97	0290	7,49	2592	8,02	2917
6,45	0,2893	6,98	0227	7,50	−0,2629	8,03	2890
		6,99	0163			8,04	2862
6,46	0,2863	7,00	0,0099	7,51	−0,2661	8,05	−0,2833
6,47	2836			7,52	2699		
6,48	2805	7,01	0,0036	7,53	2733	8,06	−0,2804
6,49	2774	7,02	−0,0028	7,54	2766	8,07	2771
6,50	0,2741	7,03	0092	7,55	−0,2797	8,08	2739
		7,04	0155			8,09	2705
6,51	0,2707	7,05	−0,0219	7,56	−0,2827	8,10	−0,2671
6,52	2673			7,57	2858		
6,53	2636	7,06	−0,0282	7,58	2885	8,11	−0,2635
6,54	2600	7,07	0346	7,59	2912	8,12	2598
6,55	0,2562	7,08	0409	7,60	−0,2938	8,13	2560
		7,09	0472			8,14	2522
6,56	0,2522	7,10	−0,0535	7,61	−0,2963	8,15	−0,2482
6,57	2483			7,62	2986		
6,58	2442	7,11	−0,0597	7,63	3009	8,16	−0,2441
6,59	2400	7,12	0659	7,64	3030	8,17	2399
6,60	0,2357	7,13	0722	7,65	−0,3050	8,18	2351
		7,14	0782			8,19	2313
6,61	0,2313	7,15	−0,0844	7,66	−0,3069	8,20	−0,2269
6,62	2269			7,67	3086		
6,63	2223	7,16	−0,0905	7,68	3103	8,21	−0,2224
6,64	2177	7,17	0965	7,69	3118	8,22	2177
6,65	0,2129	7,18	1026	7,70	−0,3132	8,23	2130
		7,19	1085			8,24	2082
6,66	0,2081	7,20	−0,1145	7,71	−0,3144	8,25	−0,2082
6,67	2033			7,72	3156		
6,68	1983	7,21	−0,1207	7,73	3166	8,26	−0,1984
6,69	1932	7,22	1266	7,74	3175	8,27	1933
6,70	0,1881			7,75	−0,3183		

x	$F(x)$	x	$F(x)$	x	$F(x)$	x	$F(x)$
8,28	—0,1882	8,71	0,0720	9,13	0,2794	9,56	0,3004
8,29	1830	8,72	0781	9,14	2824	9,57	2982
8,30	—0,1784	8,73	0842	9,15	0,2853	9,58	2958
		8,74	0904			9,59	2933
8,31	—0,1724	8,75	0,0965	9,16	0,2882	9,60	0,2907
8,32	1670			9,17	2908		
8,33	1616	8,76	0,1025	9,18	2934	9,61	0,2880
8,34	1560	8,77	1086	9,19	2959	9,62	2852
8,35	—0,1505	8,78	1145	9,20	0,2982	9,63	2823
		8,79	1204			9,64	2792
8,36	—0,1448	8,80	0,1263	9,21	0,3005	9,65	0,2761
8,37	1391			9,22	3026		
8,38	1333	8,81	0,1320	9,23	3046	9,66	0,2728
8,39	1275	8,82	1379	9,24	3065	9,67	2694
8,40	—0,1216	8,83	1436	9,25	0,3082	9,68	2660
		8,84	1493			9,69	2624
8,41	—0,1158	8,85	0,1549	9,26	0,3098	9,70	0,2587
8,42	1098			9,27	3113		
8,43	1038	8,86	0,1604	9,28	3131	9,71	0,2552
8,44	0977	8,87	1659	9,29	3140	9,72	2510
8,45	—0,0917	8,88	1713	9,30	0,3151	9,73	2470
		8,89	1766			9,74	2430
8,46	—0,0855	8,90	0,1819	9,31	0,3161	9,75	0,2388
8,47	0794			9,32	3170		
8,48	0732	8,91	0,1871	9,33	3178	9,76	0,2345
8,49	0670	8,92	1922	9,34	3184	9,77	2301
8,50	—0,0608	8,93	1973	9,35	0,3189	9,78	2245
		8,94	2025			9,79	2155
8,51	—0,0545	8,95	0,2071	9,36	0,3193	9,80	0,2108
8,52	0482			9,37	3195		
8,53	0419	8,96	0,2119	9,38	3196	9,81	0,2060
8,54	0356	8,97	2167	9,39	3196	9,82	2012
8,55	—0,0292	8,98	2213	9,40	0,3195	9,83	1963
		8,99	2258			9,84	1912
8,56	—0,0229	9,00	0,2303	9,41	0,3192	9,85	0,1861
8,57	0166			9,42	3187		
8,58	0102			9,43	3187	9,86	0,1810
8,59	—0,0038	9,01	0,2347	9,44	3177	9,87	1809
8,60	0,0025	9,02	2390	9,45	0,3170	9,88	1753
		9,03	2431			9,89	1710
8,61	0,0089	9,04	2472	9,46	0,3161	9,90	0,1656
8,62	0153	9,05	0,2512	9,47	3151	9,91	0,1608
8,63	0216			9,48	3139	9,92	1554
8,64	0280	9,06	0,2551	9,49	3127	9,93	1490
8,65	0,0323	9,07	2589	9,50	0,3113	9,94	1433
		9,08	2626			9,95	0,1376
8,66	0,0406	9,09	2661	9,51	0,3098		
8,67	0469	9,10	0,2696	9,52	3081	9,96	0,1319
8,68	0532			9,53	3064	9,97	1260
8,69	0595	9,11	0,2730	9,54	3045	9,98	1201
8,70	0,0657	9,12	2762	9,55	0,3085	9,99	1142
						10,00	0,1082